NATIONAL ADVISORY COMMITTEE FOR AERONAUTICS

TECHNICAL NOTE 1984

A SEMIEMPIRICAL METHOD FOR ESTIMATING THE ROLLING

MOMENT DUE TO YAWING OF AIRPLANES

By John P. Campbell and Alex Goodman

Langley Aeronautical Laboratory
Langley Air Force Base, Va.

NATIONAL ADVISORY COMMITTEE FOR AERONAUTICS

TECHNICAL NOTE 1984

A SEMIEMPIRICAL METHOD FOR ESTIMATING THE ROLLING

MOMENT DUE TO YAWING OF AIRPLANES

By John P. Campbell and Alex Goodman

SUMMARY

A method is presented for estimating the rolling moment due to yawing of airplanes. The results are given in terms of the derivative C_{l_r}, which is defined as the rate of change of rolling-moment coefficient with yawing-velocity parameter. The method is semiempirical in that it provides for experimentally determined correction factors to be applied to the theory. The correction factor for the wing is the incremental value of the rolling moment due to sideslip C_{l_β} obtained by subtracting the experimental value of C_{l_β} from the theoretical value. This incremental value of C_{l_β}, which is expressed in radians, is added to the theoretical value of C_{l_r} to give the corrected value of C_{l_r} for the wing. Similar use is made of experimental data to estimate the contribution of the vertical tail to C_{l_r}.

Comparisons of experimental and estimated values of C_{l_r} for 22 different wing configurations and 8 complete models indicate that this method provides a substantial improvement over existing theoretical methods for estimating C_{l_r}.

INTRODUCTION

Comparisons of theoretically and experimentally determined values of the rate of change of the rolling-moment coefficient with the yawing-velocity parameter C_{l_r} (referred to as the rolling moment due

to yawing) have indicated that the theory of reference 1 is inadequate for estimating C_{l_r}, especially in the case of swept wings. (See references 1 and 2.) The largest discrepancies between theory and experiment occur at moderate and high lift coefficients and are attributed to the fact that the theory is based on potential-flow concepts and thus does not account for the partial flow separation which usually exists on swept wings even at moderate angles of attack. A study has therefore been made to find a method of estimating C_{l_r} which does take into account this partial flow separation. In one promising method found in this study, use is made of the similarity between C_{l_r} and the derivative C_{l_β}, the rolling moment due to sideslip. A description of the method and a comparison of experimental values of C_{l_r} and values estimated by this method are given in the present paper.

The method of estimating C_{l_r} presented herein is semiempirical in that it necessitates an experimentally determined correction factor to be applied to theory. The correction factor for the wing is merely the incremental value of C_{l_β} obtained by subtracting the experimental value of C_{l_β} from the theoretical value (reference 1) for the given wing at the same lift coefficient. This incremental value of C_{l_β}, expressed in radians, is then added to the theoretical value of C_{l_r} obtained from reference 1 to give the corrected value of C_{l_r} for the wing. Similar use is made of experimental data to estimate the tail contribution to C_{l_r}.

One advantage of this method is that lateral-stability force-test data are usually available for obtaining the experimental values of C_{l_β} for the particular airplane under consideration. Another advantage is that the correction factor can be based on an experimental value of C_{l_β} obtained from force tests made at much higher values of Reynolds number and Mach number than can be reached with existing equipment for measuring C_{l_r}.

SYMBOLS

The symbols used in the analysis and in the presentation of the results are defined herein. The data presented are referred in all cases to the stability system of axes.

C_L lift coefficient $\left(\dfrac{\text{Lift}}{\frac{1}{2}\rho V^2 S}\right)$

C_l rolling-moment coefficient $\left(\dfrac{\text{Rolling moment}}{\frac{1}{2}\rho V^2 Sb}\right)$

C_Y lateral-force coefficient $\left(\dfrac{\text{Lateral force}}{\frac{1}{2}\rho V^2 S}\right)$

$C_{l_r} = \dfrac{\partial C_l}{\partial \frac{rb}{2V}}$

$C_{l_\beta} = \dfrac{\partial C_l}{\partial \beta}$

$C_{Y_\beta} = \dfrac{\partial C_Y}{\partial \beta}$

ρ mass density of air, slugs per cubic foot

S wing area, square feet

V airspeed, feet per second

$\bar{c}$ wing mean chord, feet (b/A)

b wing span, feet

$\bar{x}$ longitudinal distance rearward from airplane center of gravity to wing aerodynamic center, feet

l longitudinal distance rearward from center of gravity to center of pressure of vertical tail, measured parallel to longitudinal stability axis, feet

z vertical distance upward from center of gravity to center of pressure of vertical tail measured perpendicular to longitudinal stability axis, feet

Λ sweep angle of wing quarter chord line (positive for sweepback), degrees

A aspect ratio (b^2/S)

$\dfrac{rb}{2V}$ yawing–velocity parameter

r yawing angular velocity, radians per second

α angle of attack, degrees

β angle of sideslip, radians

a_o section-lift-curve slope, radians

λ taper ratio $\left(\dfrac{\text{Tip chord}}{\text{Root chord}}\right)$

Γ dihedral angle, degrees

ANALYSIS AND METHOD

Contribution of Wing to C_{l_r}

Analysis of the experimental data presented in references 1 and 2 and of similar data from other investigations conducted by the NACA indicates that the discrepancies between theoretical and experimental values of C_{l_r} for wings are quite similar to the discrepancies between theoretical and experimental values of C_{l_β}. Typical data which illustrate this point are presented in figure 1. For both C_{l_r} and C_{l_β} only moderate disagreements between theory and experiment exist at low lift coefficients, but very large disagreements usually

occur at the higher lift coefficients for swept wings. As stated previously, the large difference between theory and experiment at moderate and high lift coefficients for swept wings is probably caused by partial flow separation over the wing that is not accounted for by theory.

The observed similarity between C_{l_r} and C_{l_β} of the wing, regarding the comparison of theory and experiment, is approximately expressed by the equation

$$C_{l_{r_{exp}}} - C_L \left(\frac{C_{l_r}}{C_L}\right)_{theory} = - C_{l_{\beta_{exp}}} + C_L \left(\frac{C_{l_\beta}}{C_L}\right)_{theory} \tag{1}$$

where both C_{l_r} and C_{l_β} are expressed in terms of radians.

Rearranging this expression gives the following equation for estimating the contribution of the wing to C_{l_r}

$$C_{l_{r_{wing}}} = C_L \left(\frac{C_{l_r}}{C_L}\right)_{theory} + C_L \left(\frac{C_{l_\beta}}{C_L}\right)_{theory} - C_{l_{\beta_{exp}}} \tag{2}$$

The experimental value of C_{l_β} can be obtained from lateral–stability force–test data for the wing under consideration. Theoretical values of C_{l_r}/C_L and C_{l_β}/C_L can be obtained from the formulas and charts of reference 1. For convenience, two of the estimation charts of reference 1 for a taper ratio of 1.0 are presented in figures 2 and 3 of the present paper. Values of C_{l_r}/C_L and C_{l_β}/C_L for taper ratios of 0.25 and 0.50 can be calculated by the methods described in reference 1.

Contribution of Vertical Tail to C_{l_r}

In order to obtain the values of C_{l_r} for a complete airplane it is of course necessary to add the contributions of the vertical tail, fuselage, and perhaps other components to the value obtained for the wing alone. Usually the fuselage contribution is neglected and the vertical-tail contribution is assumed to be

$$\Delta C_{l_{r_{tail}}} = -2\frac{l}{b}\frac{z}{b}\Delta C_{Y_{\beta_{tail}}} \tag{3}$$

where l, z, and b are determined from the geometry of the airplane and $\Delta C_{Y_{\beta_{tail}}}$ is obtained from lateral-stability force-test data or, if such data are not available, from conventional estimation procedures.

The contribution of the vertical tail to C_{l_β} can be estimated from a similar equation:

$$\Delta C_{l_{\beta_{tail}}} = \frac{z}{b}\Delta C_{Y_{\beta_{tail}}} \tag{4}$$

Dividing (3) by (4) and rearranging gives

$$\Delta C_{l_{r_{tail}}} = -2\frac{l}{b}\Delta C_{l_{\beta_{tail}}} \tag{5}$$

If force-test data are available for determining $\Delta C_{l_{\beta_{tail}}}$, equation (5) is probably more reliable than equation (3) because it takes into account any interference effects that might cause the effective vertical location of the center of pressure of the tail to be different from the location determined from geometrical procedures.

Equation (5) indicates that if the factor l/b has a value of 0.5, $\Delta C_{l_{r_{tail}}}$ is equal to $-\Delta C_{l_{\beta_{tail}}}$. In many cases the value of l/b is approximately 0.5, and in these cases equation (2) can be adapted to estimate the C_{l_r} of the complete airplane by using for $C_{l_{\beta_{exp}}}$ the experimental value of C_{l_β} for the complete airplane instead of C_{l_β} for the wing alone. For cases in which l/b is not approximately 0.5, however, equation (5) should be used to estimate the tail contribution to C_{l_r} and equation (2) the wing contribution.

EXPERIMENTAL VERIFICATION OF METHOD

In order to check the method, experimental values of C_{l_r} for the 22 different wing configurations listed in table I and 8 complete models listed in table II have been compared with values of C_{l_r} given by equations (2) and (5). The results of the comparison are presented in figures 4 to 18. Also shown in these figures are experimental values of C_{l_β} and the theoretical values of C_{l_β} and C_{l_r} obtained from reference 1. The experimental results for the 22 wings include data which show the effects of systematic variations of aspect ratio, sweepback, and taper ratio and the effects of changes in airfoil section, flap configuration, and geometric dihedral angle. None of the complete models for which results are presented was equipped with a horizontal tail.

Wings

The comparisons of estimated and experimental values of C_{l_r} for wings 1 to 10, which are shown in figures 4 to 8, generally indicate fair to good agreement except for the wings of aspect ratio 1.34. Even in the cases where quantitative agreement is not obtained, the trend of the variation of C_{l_r} with lift coefficient is indicated by the estimated values. A comparison of the results for wings 5 and 10 (figs. 6 and 8, respectively), which have the same plan form except that one is swept back and the other swept forward, shows that the present method satisfactorily predicts the different effect of partial flow separation over the wing in the two cases — a decrease in C_{l_r} for the sweptback wing and an increase in C_{l_r} for the sweptforward wing.

The results for wings 5, 11, 12, and 13, presented in figures 6, 9, and 10, show that the agreement between the experimental and estimated values is not quite so good for the tapered wings (wings 11, 12, and 13) as for the untapered wing (wing 5). The trends in the variation of C_{l_r}, however, are clearly shown by the estimated values. The results for wing 14, which has a taper ratio of 0, show good agreement between the estimated and experimental values of C_{l_r}. Theoretical values of C_{l_r}/C_L and C_{l_β}/C_L for a taper ratio of 0.25 were used in making the estimate

for wing 14 since values of C_{l_r}/C_L for a wing having a taper ratio of 0 and an aspect ratio as high as 2.31 were not available from the present theories.

The results for wings 5, 15, and 16, presented in figures 6 and 11, show that the present method (equation (2)) predicts the effects of airfoil section on the variation of C_{l_r} with lift coefficient. The estimated values are in good agreement with the measured values in showing that, as the airfoil section is changed from an NACA 0012 to an NACA 65_1–012 and then to a 12–percent–thick biconvex section, the maximum value of C_{l_r} becomes progressively smaller and the departure from a linear variation of C_{l_r} with C_L occurs at progressively lower lift coefficients.

The results presented in figure 12 for the wings with dihedral (wings 17 and 18) show that although equation (2) gives values that are in fair agreement with the experimental results, the agreement is not so good as for the same wing with 0° dihedral (wing 5). The theory of reference 1 was not corrected to account for dihedral because no satisfactory theoretical method of correcting C_{l_r} for dihedral has been developed. (See reference 3.) Even though theoretical values for 0° dihedral are used, however, the present estimation method appears to account satisfactorily for the opposite effects of positive and negative dihedral on C_{l_r}.

The comparisons of experimental and estimated results for four flapped wing configurations (wings 19 to 22) are shown in figures 13 and 14. Good quantitative agreement is indicated for wings 20 and 21, whereas qualitative agreement regarding the trend of the variation of C_{l_r} with C_L is shown for the other two wings. The discrepancies at zero lift between the experimental and theoretical (reference 1) values of both C_{l_r} and C_{l_β} for the wings with 0.9 span split flaps (wings 20 and 22) are attributed partly to the fact that at zero lift these wings are at a negative angle of attack which (because of the sweepback) causes the wings to have effectively a positive dihedral angle. For example, the discrepancies at low lift coefficients between theory and experiment for both C_{l_r} and C_{l_β} are about the same for wing 20 as for wing 17 which has a dihedral angle of 10°. In the case of the wing with the 0.4 span flaps (wing 19) at zero lift, an effect opposite to that for wing 18 occurs because, even though the wing is at a negative angle of attack and therefore effectively has positive dihedral, the part of the wing outboard of the flap is producing negative lift and thus tends to give values of C_{l_β} and C_{l_r}

opposite in sign to those obtained at positive lift coefficients. No
discrepancy exists at zero lift for the wing with nose flaps (wing 21)
because this wing, like the unflapped wing (wing 5), gives zero lift
at zero angle of attack. For all four of the flapped wings, the
discrepancies that occur at low as well as at high lift coefficients
are accounted for, at least qualitatively, by equation (2).

Complete Models

Comparisons of experimental and estimated values of C_{l_r} for the
eight complete models are presented in figures 15 to 18. For the
estimated values, the C_{l_r} for the vertical-tail-off condition was
determined from equation (2) and the contribution of the vertical tail
was determined from equation (5). Although equation (2) was intended
to be used only for estimating the wing contribution, it was used in
these cases to estimate the values of C_{l_r} for the wing-fuselage
combination because the contribution of the fuselage is slight and is
usually neglected. When equation (5) was used to estimate the tail
contribution, the variation of l/b with angle of attack was taken
into account.

The results for models 1 and 2 (fig. 15) indicate that equation (2)
is satisfactory for estimating the wing-fuselage contribution to C_{l_r}
and that equation (5) gives a satisfactory prediction of the tail
contribution so that the estimates for the complete models are in
fairly good agreement with the experimental data. Since models 1 and 2
are equipped with wing 14, the effect of the fuselage on C_{l_r} for
these models can be ascertained by a comparison of the data of figure 10
(wing 14) with the tail-off data of figure 15. This comparison indicates
that the effect of the fuselage in these cases was quite small. At
zero lift coefficient, models 1 and 2 have identical values of C_{l_β},
but because of the different tail lengths (table II) the value of C_{l_r}
for model 1 is less than half that of model 2. The good agreement
between estimated and experimental values of C_{l_r} at zero lift indicate
that equation (5) satisfactorily accounts for this difference in tail
length.

The agreement of estimated and experimental results for model 3
(fig. 16), is not so good as for models 1 and 2. Since these three
models have the same wing-fuselage combination, the poorer agreement

in the case of model 3 is apparently caused by an overestimation of the tail contribution.

In the case of model 4, which is equipped with wing 5, the agreement between the estimated and experimental values for the wing-fuselage combination (fig. 16) is not so good as the agreement in the case of the wing alone (fig. 6). The experimental data show that the addition of the fuselage caused a decrease in C_{l_r} throughout the lift range but did not appreciably affect C_{l_β}. This fact accounts for the disagreement in the tail-off case for model 4. Since the disagreement in the tail-on case is about the same as that for tail off, the estimate of the tail contribution appears satisfactory for this model.

The agreement between estimated and experimental values of C_{l_r} for models 5 and 6 (fig. 17) is very good over the lift range for both the tail-off and tail-on conditions. These models had the same fuselage and wing (wing 13) but had vertical tails of different size. The close agreement between estimated and experimental values for these two models is surprising in view of the disagreement indicated at the higher lift coefficients for the wing alone (wing 13, fig. 10). The data for models 5 and 6 are probably more reliable than the data for wing 13 because the model data were obtained from several tests, all of which showed similar results, whereas the wing alone data were obtained from a single test.

Results are presented in figure 18 for models 7 and 8 which have the same wing and vertical tail area as model 5 but which have different fuselage lengths and different values of l/b. The results for model 7, which has the short fuselage, show good agreement between the calculated and experimental values. In the case of the model with the long fuselage (model 8), however, the estimated values are generally higher than the experimental values for both the tail-off and tail-on conditions. As in the case of models 5 and 6, the agreement between estimated and measured values for models 7 and 8 is better than for the corresponding wing alone (wing 13) at the higher lift coefficients.

CONCLUDING REMARKS

On the basis of the comparisons of experimental and estimated values of C_{l_r} for the 22 different wing configurations and 8 complete models, the procedure presented for estimating the rolling moment due to yawing appears to provide a substantial improvement over existing theoretical methods.

Langley Aeronautical Laboratory
        National Advisory Committee for Aeronautics
                Langley Air Force Base, Va., September 13, 1949

REFERENCES

1. Toll, Thomas A., and Queijo, M. J.: Approximate Relations and
        Charts for Low-Speed Stability Derivatives of Swept Wings.
        NACA TN 1581, 1948.

2. Goodman, Alex, and Brewer, Jack D.: Investigation at Low Speeds
        of the Effect of Aspect Ratio and Sweep on Static and Yawing
        Stability Derivatives of Untapered Wings. NACA TN 1669, 1948.

3. Queijo, M. J., and Jaquet, Byron M.: Investigation of Effects of
        Geometric Dihedral on the Low-Speed Static Stability and Yawing
        Characteristics of an Untapered 45° Sweptback-Wing Model of
        Aspect Ratio 2.61. NACA TN 1668, 1948.

TABLE I

SUMMARY OF PERTINENT INFORMATION REGARDING WINGS CONSIDERED IN ANALYSIS

Wing	Sweep angle, Λ (deg)	Aspect ratio, A	Taper ratio, λ	Span, b (ft)	Dihedral angle, Γ (deg)	Test Reynolds number	Airfoil section	Figure	Source
1	0	1.34	1.00	2.21	0	1.58×10^6	NACA 0012	4	Reference 2
2	45	1.34	1.00	2.20	0	1.56	NACA 0012	4	
3	60	1.34	1.00	2.21	0	1.56	NACA 0012	5	
4	0	2.61	1.00	3.08	0	1.10	NACA 0012	5	
5	45	2.61	1.00	3.05	0	1.10	NACA 0012	6	
6	60	2.61	1.00	3.05	0	1.08	NACA 0012	6	
7	0	5.16	1.00	4.26	0	.78	NACA 0012	7	
8	45	5.16	1.00	4.26	0	.77	NACA 0012	7	
9	60	5.16	1.00	4.28	0	.76	NACA 0012	8	
10	45	2.61	1.00	3.05	0	1.10	NACA 0012	8	
11	45	2.61	.50	3.05	0	1.19	NACA 0012	9	NACA tests
12	45	2.61	.25	3.05	0	1.23	NACA 0012	9	
13	45	4.00	.60	3.00	0	.71	NACA 65A008	10	
14	52.2	2.31	0	3.04	0	1.62	NACA $65_{(06)}$-006.5	10	
15	45	2.61	1.00	3.05	0	1.10	NACA 65_1-012	11	Reference 3
16	45	2.61	1.00	3.05	0	1.10	12-percent biconvex	11	
17	45	2.61	1.00	3.05	10	1.10	12-percent biconvex	12	
18	45	2.61	1.00	3.05	-10	1.10	12-percent biconvex	12	
a19	45	2.61	1.00	3.05	0	1.10	NACA 0012	13	NACA tests
b20	45	2.61	1.00	3.05	0	1.10	NACA 0012	13	
c21	45	2.61	1.00	3.05	0	1.10	NACA 0012	14	
d22	45	2.61	1.00	3.05	0	1.10	NACA 0012	14	
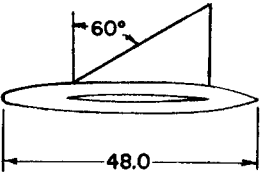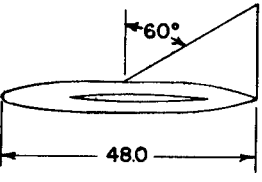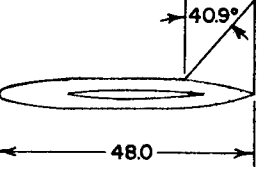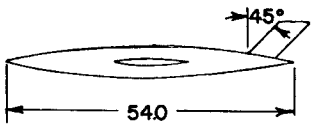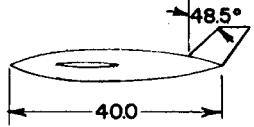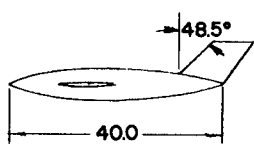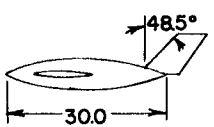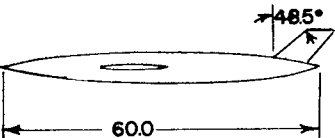
aWing with 0.4 span split flaps.
bWing with 0.9 span split flaps.
cWing with nose flaps.
dWing with nose and 0.9 span split flaps.

TABLE II

SUMMARY OF PERTINENT INFORMATION REGARDING COMPLETE MODELS CONSIDERED IN ANALYSIS

Model	Side elevation (Dimensions in inches)	Wing aspect ratio	Fineness ratio of fuselage	Vertical tail aspect ratio	$\dfrac{\text{Tail area}}{\text{Wing area}}$	$\left(\dfrac{l}{b}\right)_{\alpha=0^{\circ}}$ (d)	$\left(\dfrac{z}{b}\right)_{\alpha=0^{\circ}}$ (d)
1	60° 48.0	[a]2.31	7.38	1.15	0.500	0.144	0.167
2	60° 48.0	[a]2.31	7.38	1.15	.500	.392	.167
3	40.9° 48.0	[a]2.31	7.38	2.31	.250	.572	.167
4	45° 54.0	[b]2.61	8.34	1.29	.100	.576	.110
5	48.5° 40.0	[c]4.00	6.67	1.00	.150	.464	.089
6	48.5° 40.0	[c]4.00	6.67	1.00	.225	.464	.108
7	48.5° 30.0	[c]4.00	5.00	1.00	.150	.347	.089
8	48.5° 60.0	[c]4.00	10.00	1.00	.150	.697	.089

[a]Same wing as wing 14, table I.
[b]Same wing as wing 5, table I.
[c]Same wing as wing 13, table I.

[d]Center of pressure of the triangular vertical tails was assumed to be the center of tail area for models 1 to 3 and for the trapezoidal tails the 25-percent station of the tail mean aerodynamic chord for models 4 to 8.
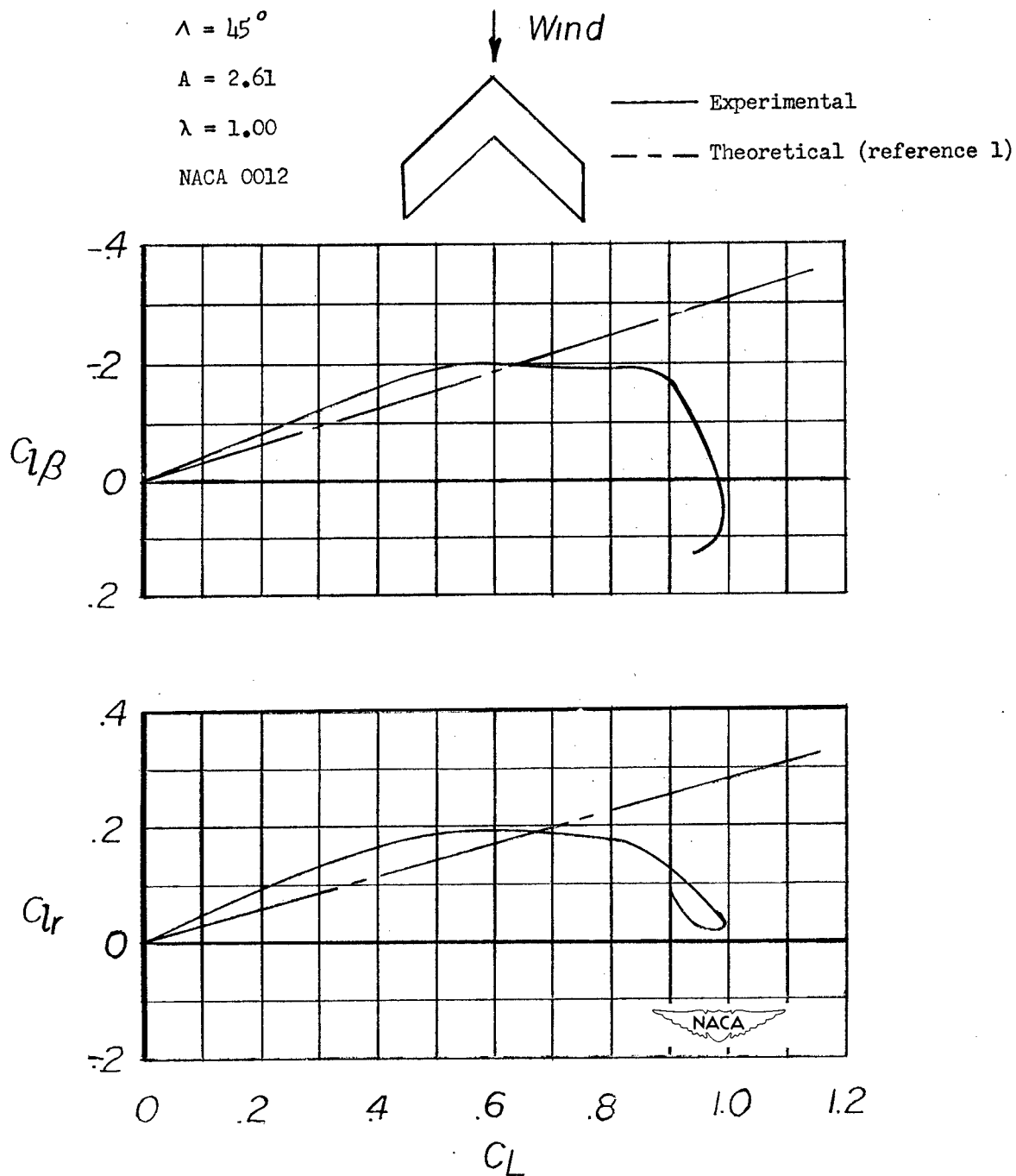
Figure 1.- Variation of C_{l_β} and C_{l_r} with lift coefficient for a 45° sweptback wing.
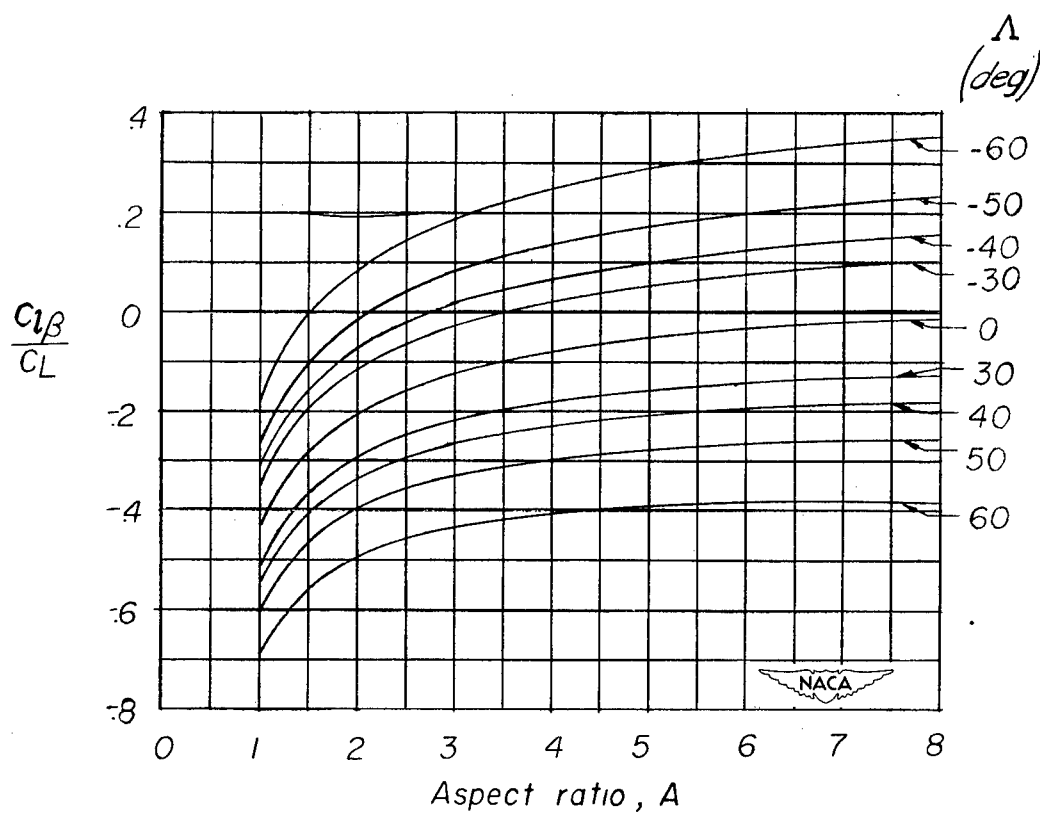
Figure 2.- Variation of the rolling moment due to sideslip with aspect
ratio for various sweep angles. $a_0 = 5.67$; $\lambda = 1.0$. (Reference 1)
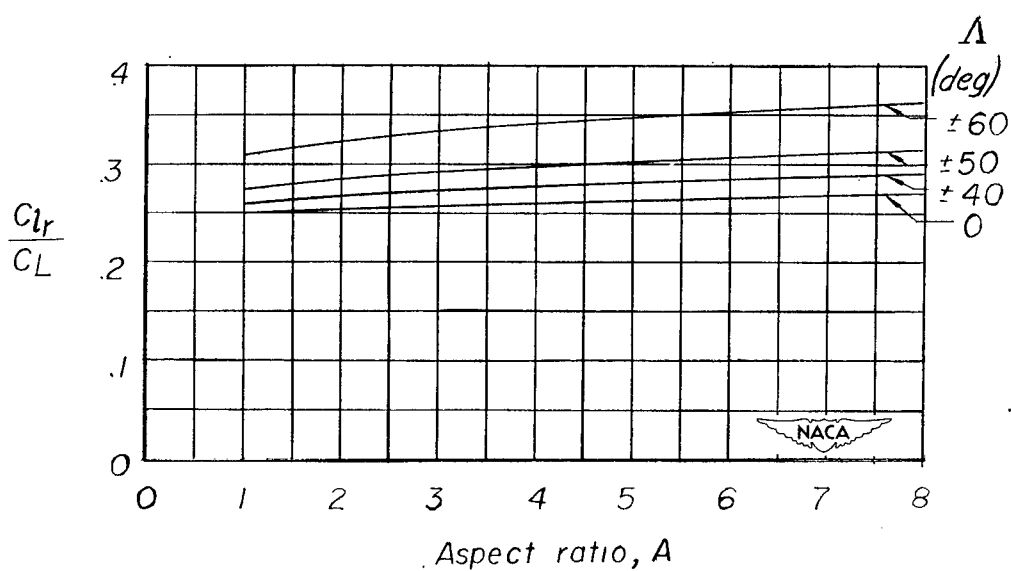
Figure 3.- Variation of the rolling moment due to yawing with aspect
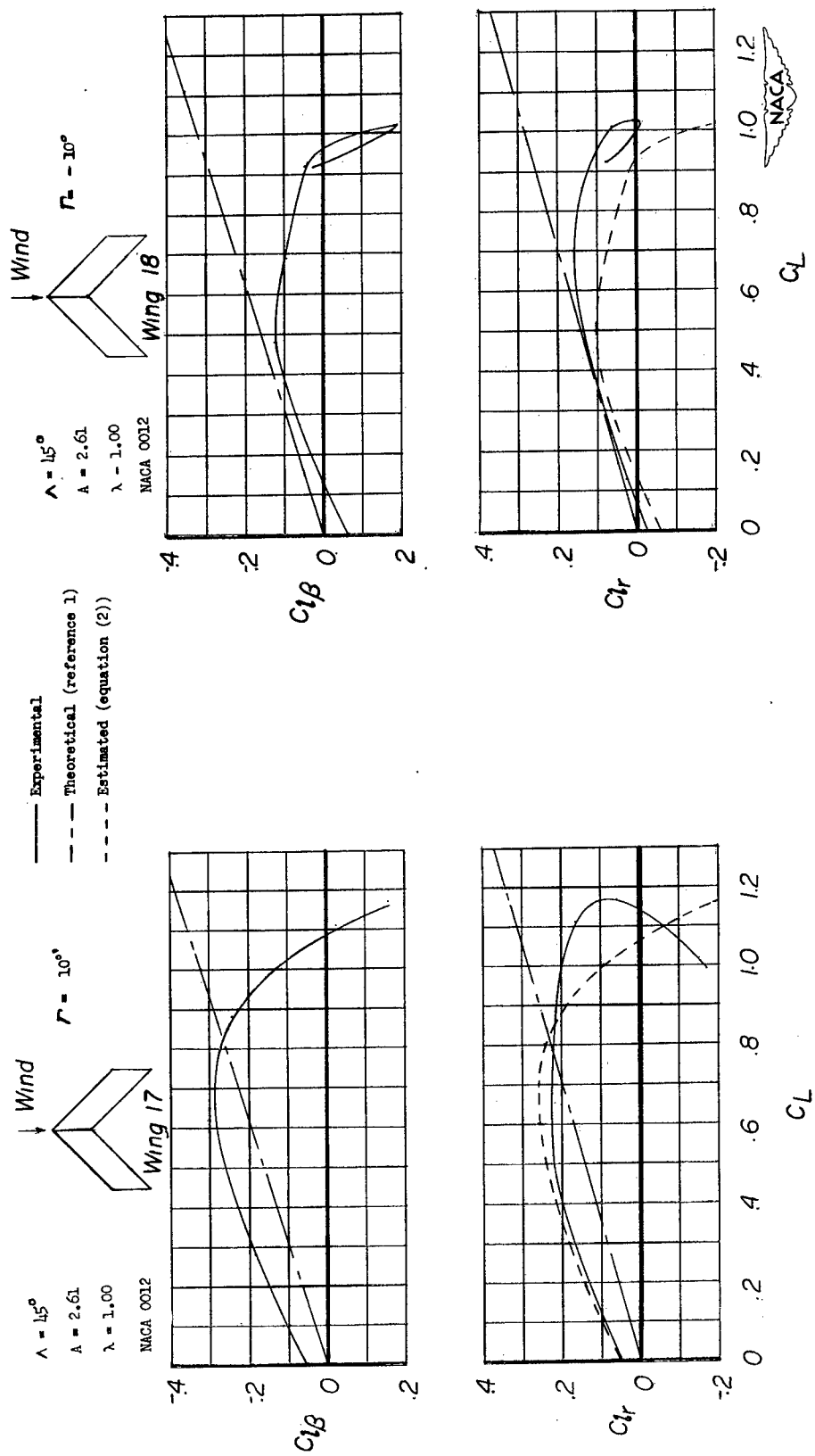ratio for various sweep angles. $\lambda = 1.0$; $\dfrac{\bar{x}}{c} = 0$. (Reference 1)
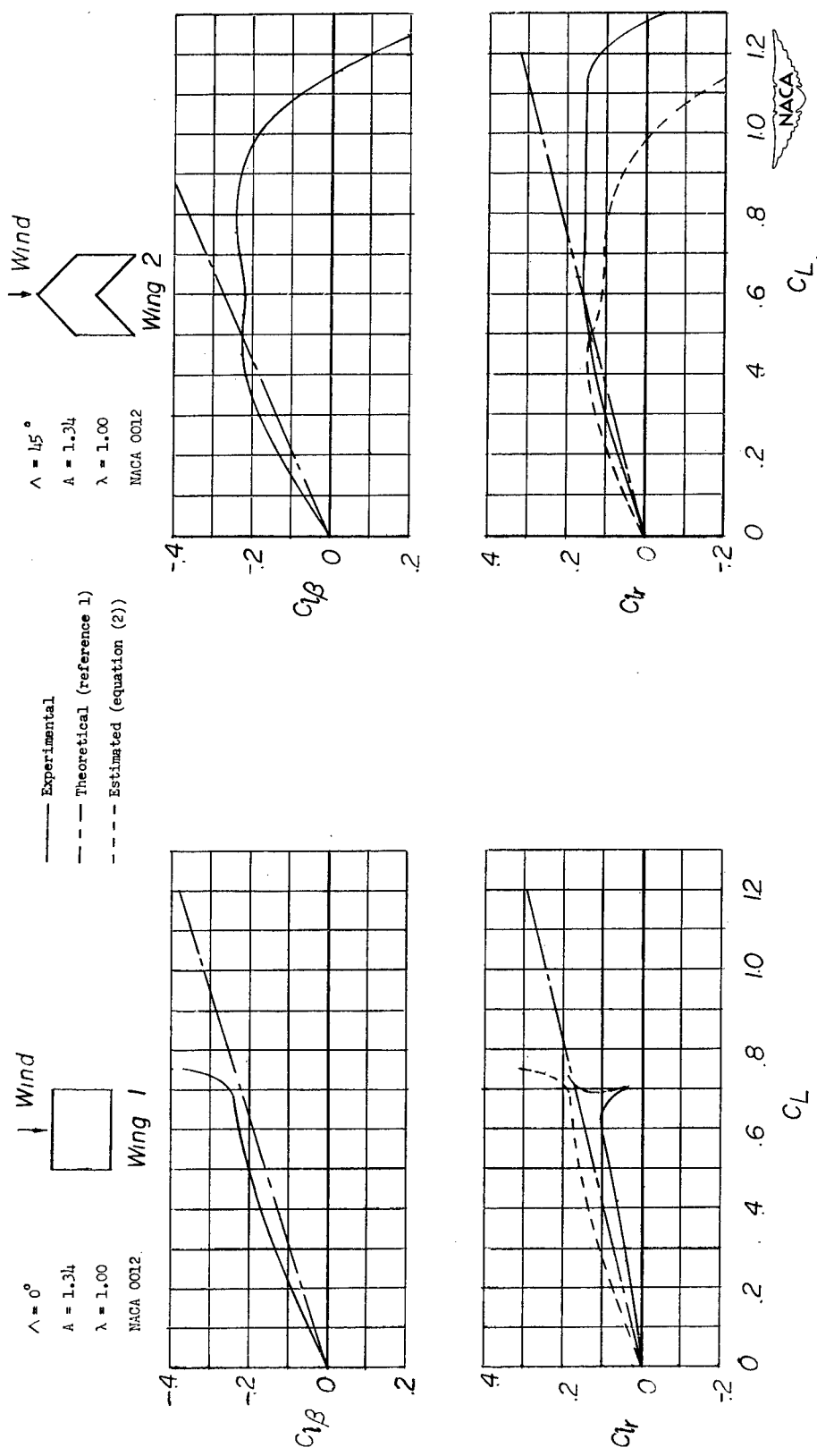
Figure 4.- Estimation of the rolling moment due to yawing for wings 1 and 2.
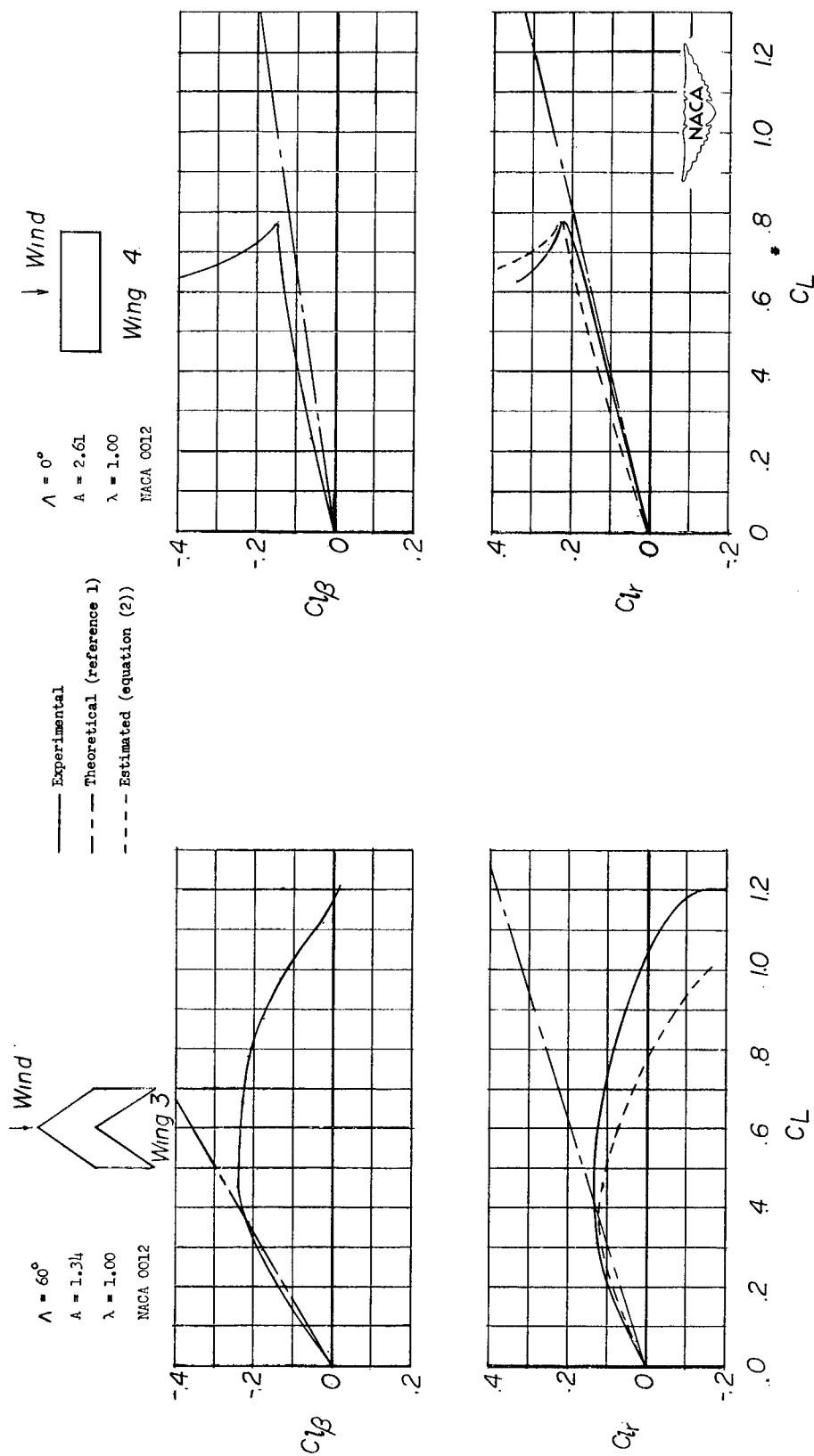
Figure 5.- Estimation of the rolling moment due to yawing for wings 3 and 4.
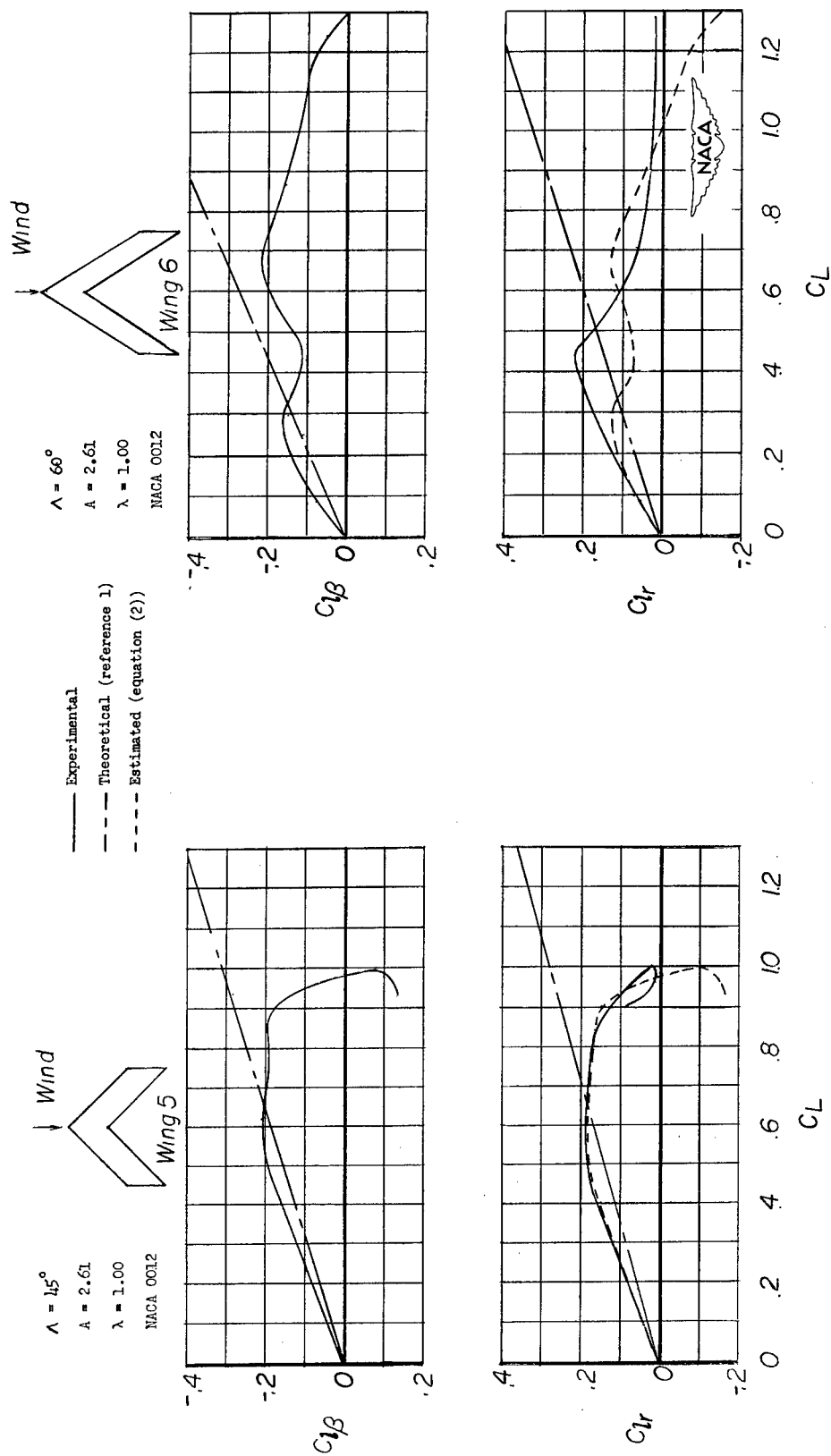
Figure 6.- Estimation of the rolling moment due to yawing for wings 5 and 6.
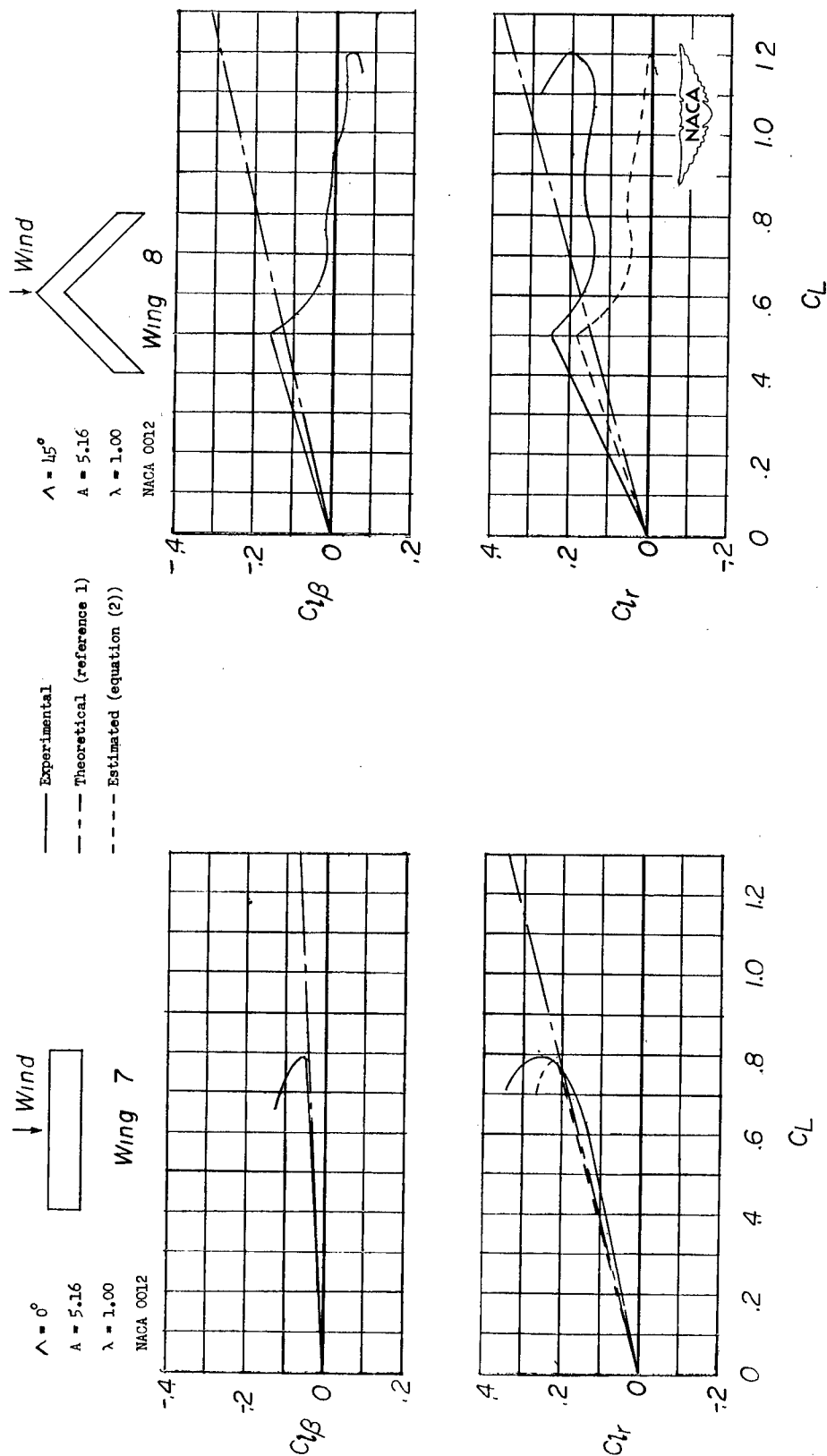
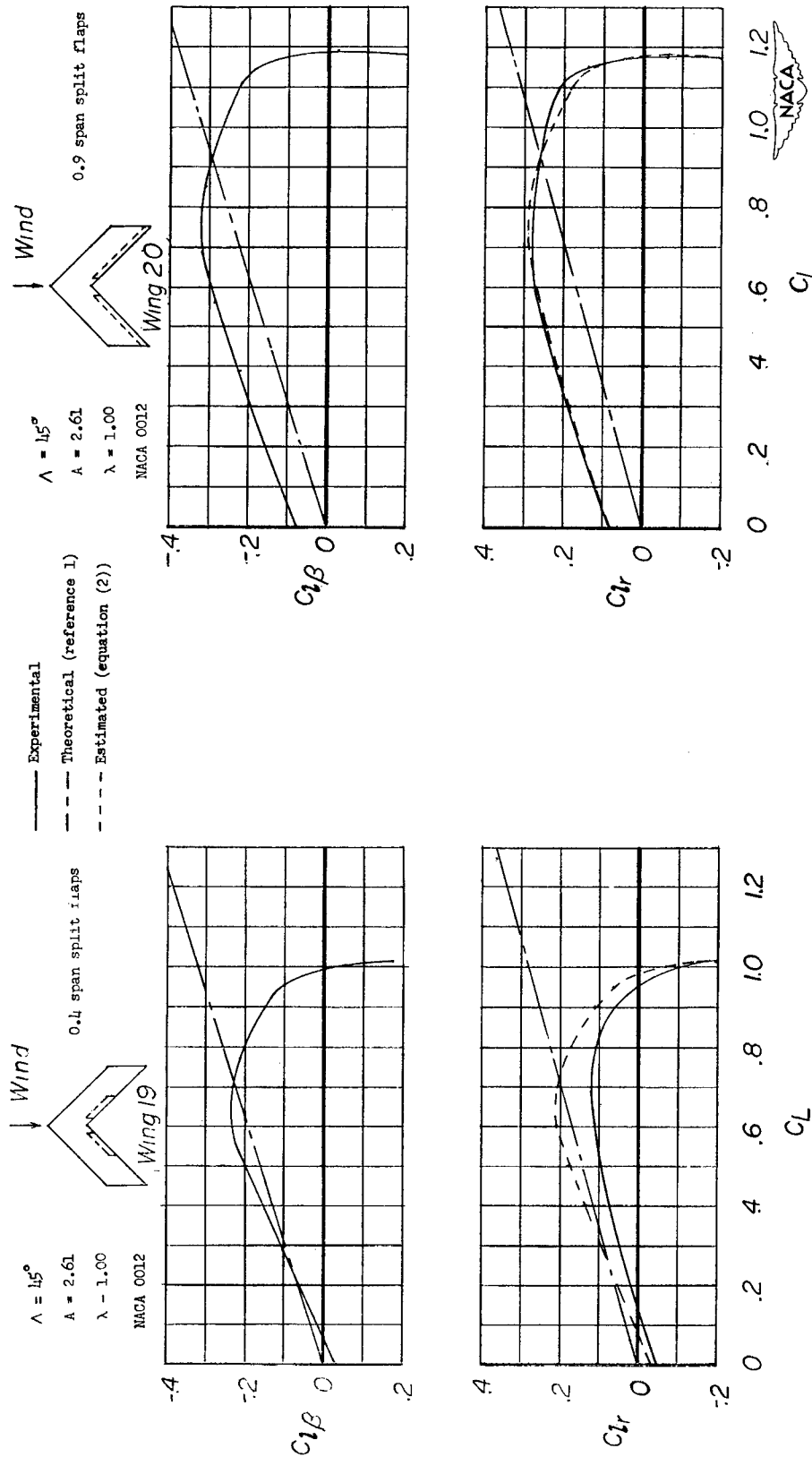Figure 7.- Estimation of the rolling moment due to yawing for wings 7 and 8.
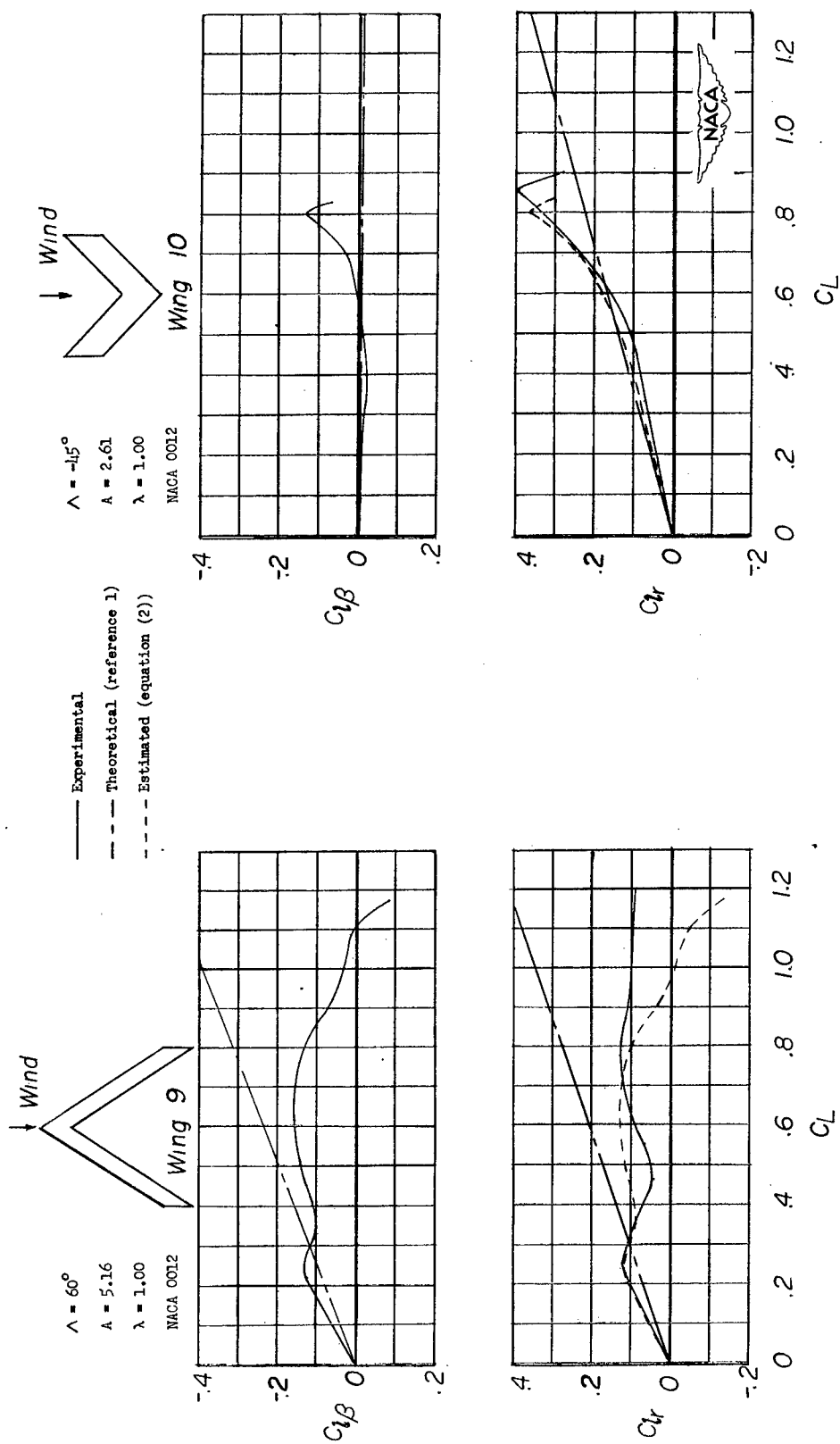
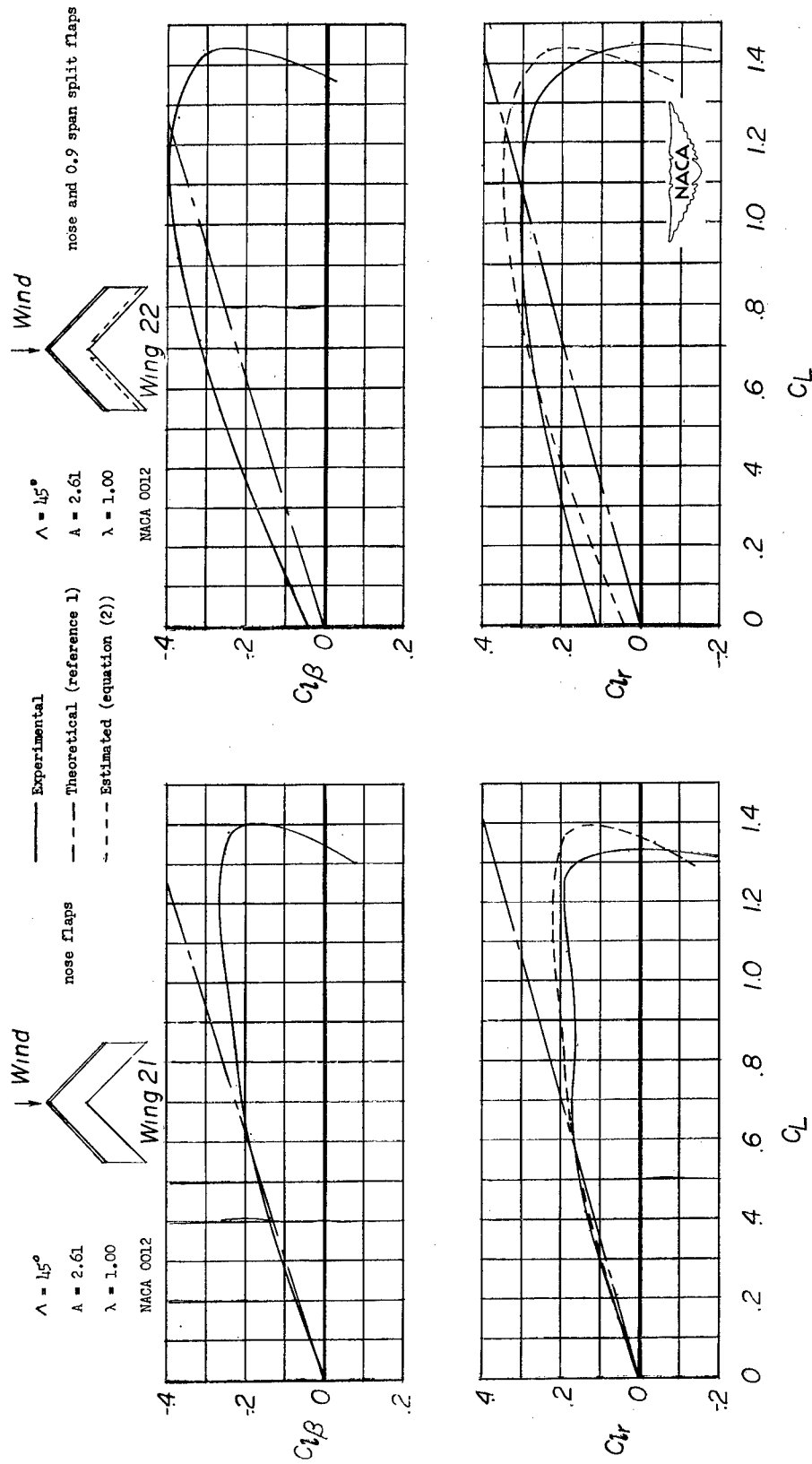Figure 8.- Estimation of the rolling moment due to yawing for wings 9 and 10.
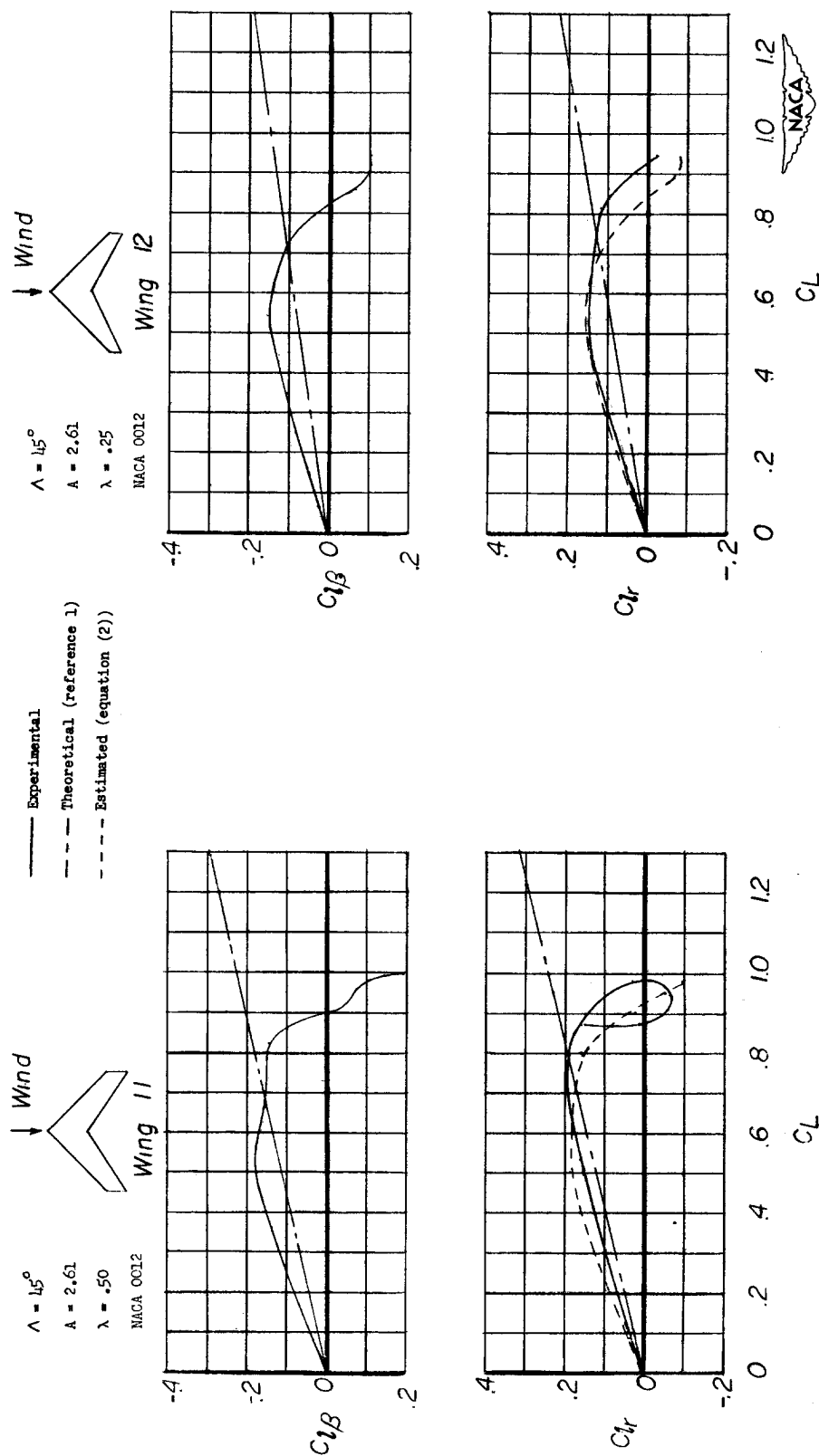
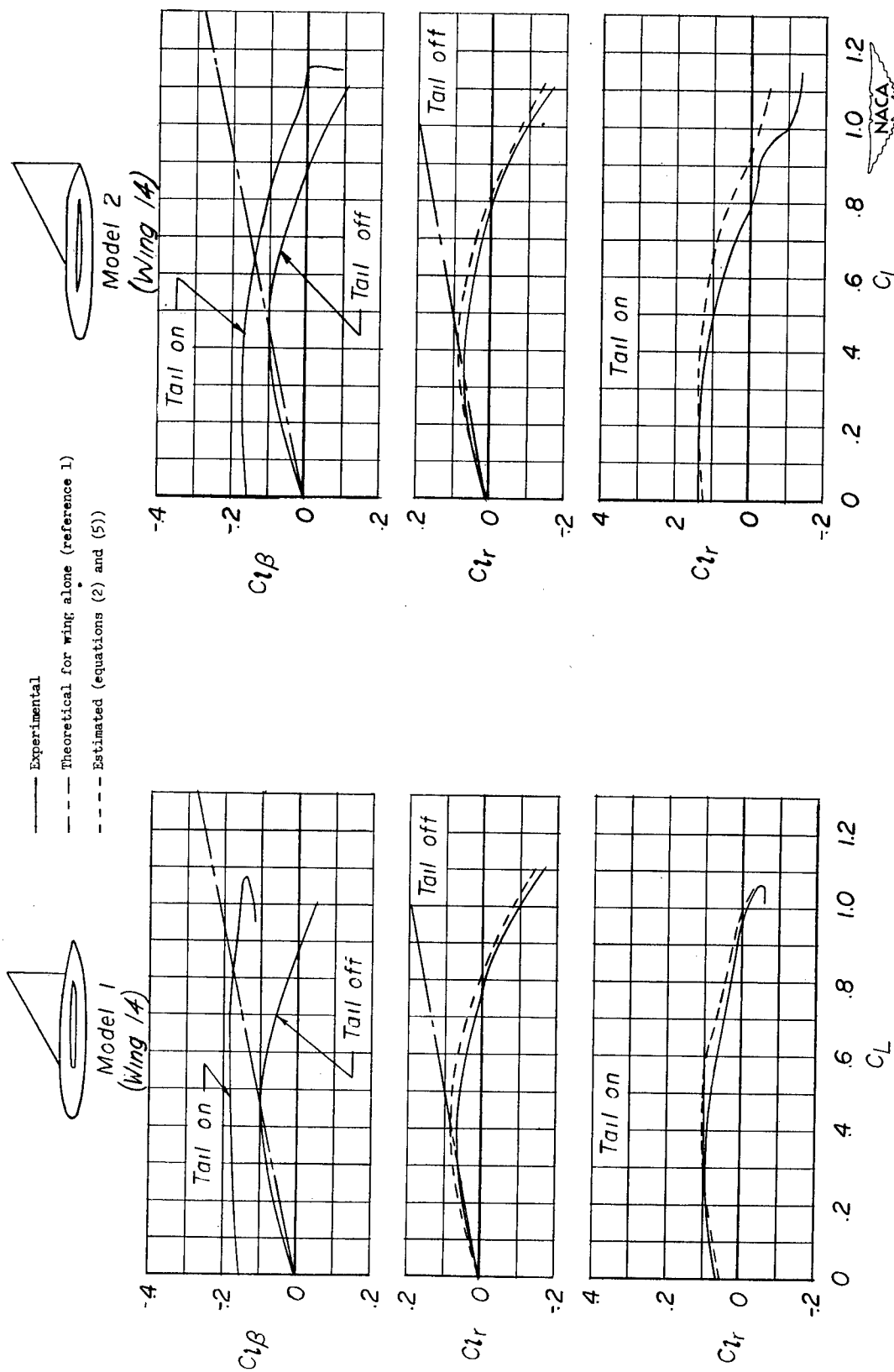Figure 9.- Estimation of the rolling moment due to yawing for wings, 11 and 12.
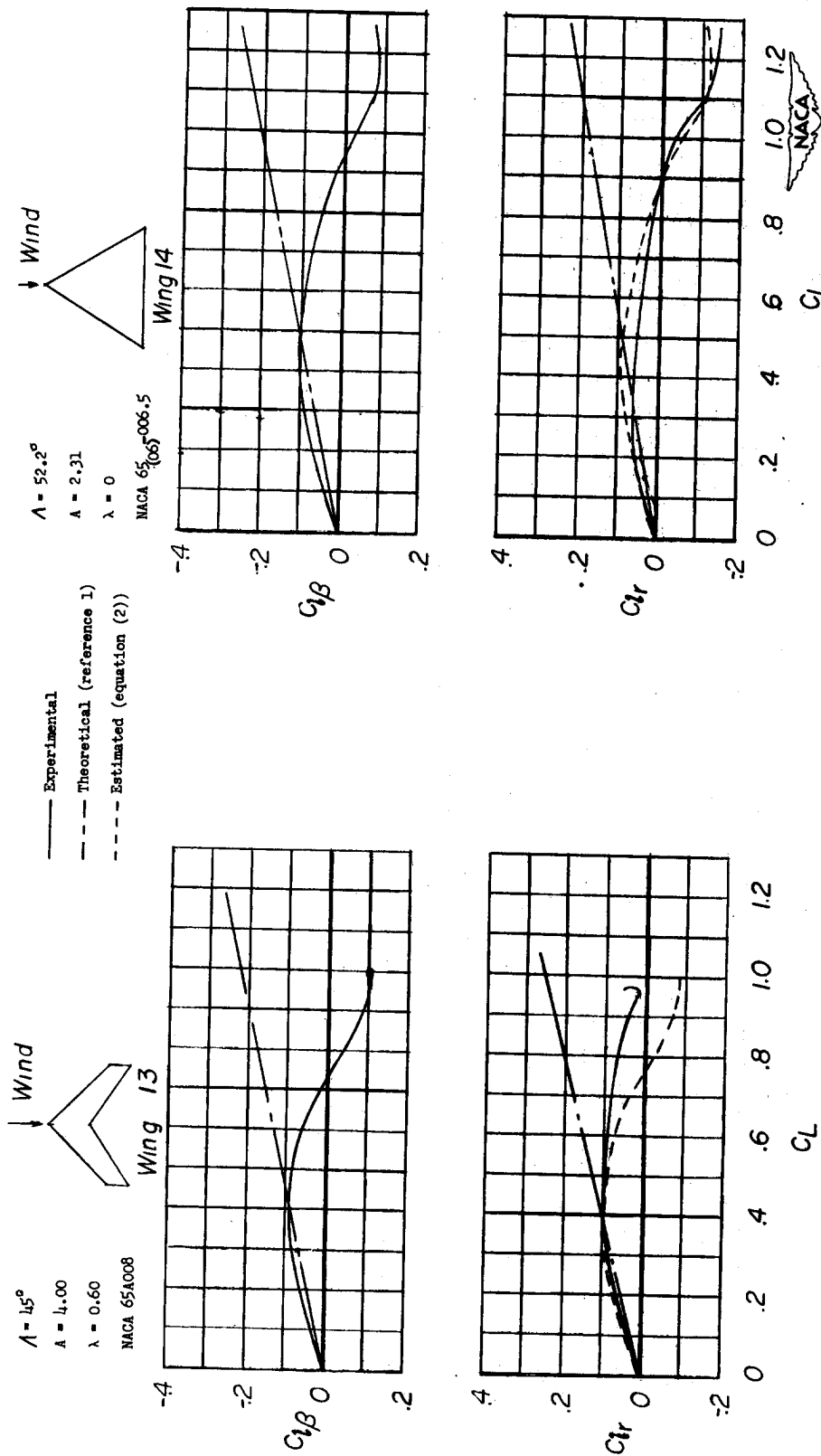
Figure 10.- Estimation of the rolling moment due to yawing for wings 13 and 14.
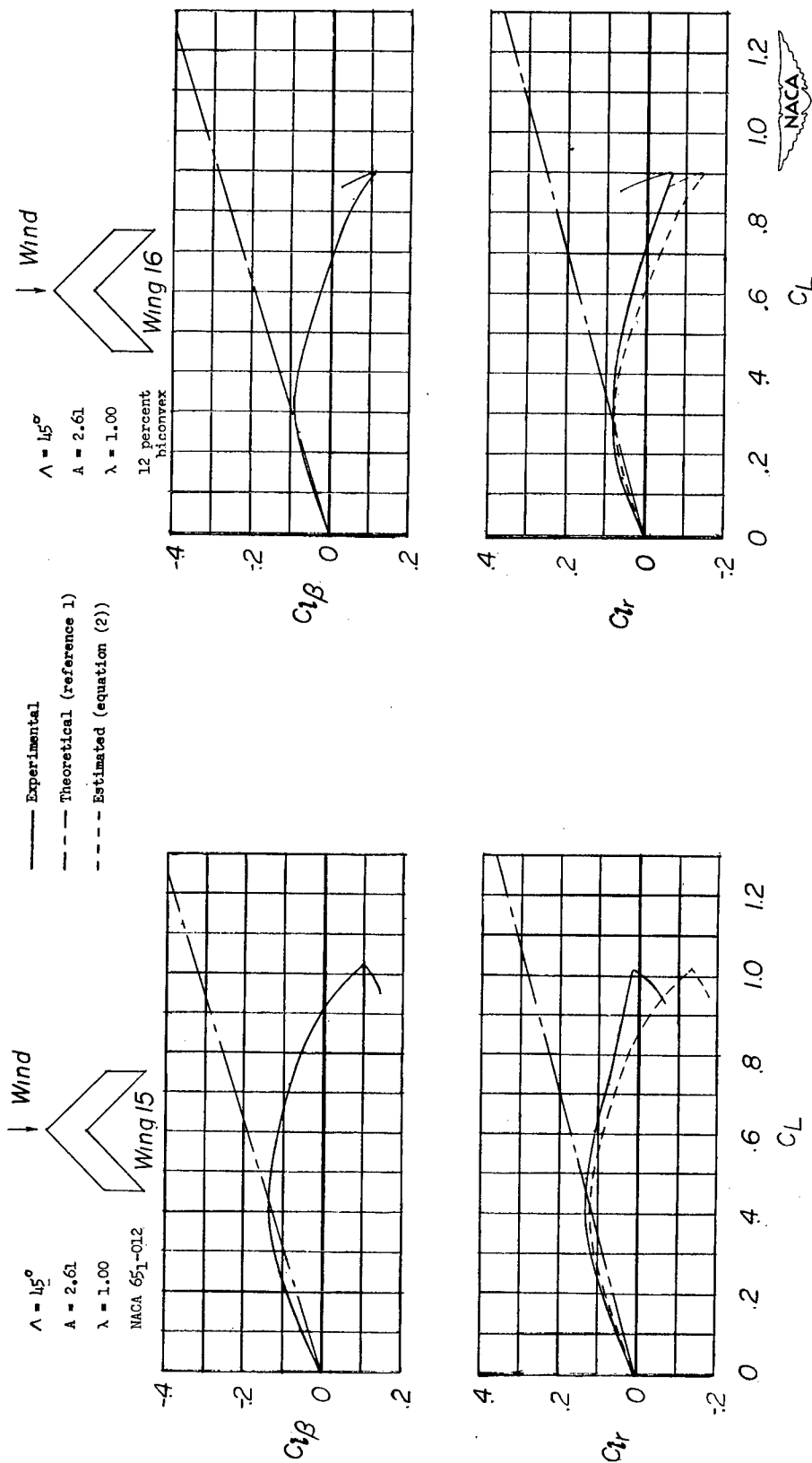
Figure 11.- Estimation of the rolling moment due to yawing for wings 15 and 16.

Figure 12.- Estimation of the rolling moment due to yawing for wings 17 and 18.

Figure 13.- Estimation of the rolling moment due to yawing for wings 19 and 20.

Figure 14.- Estimation of the rolling moment due to yawing for wings 21 and 22.

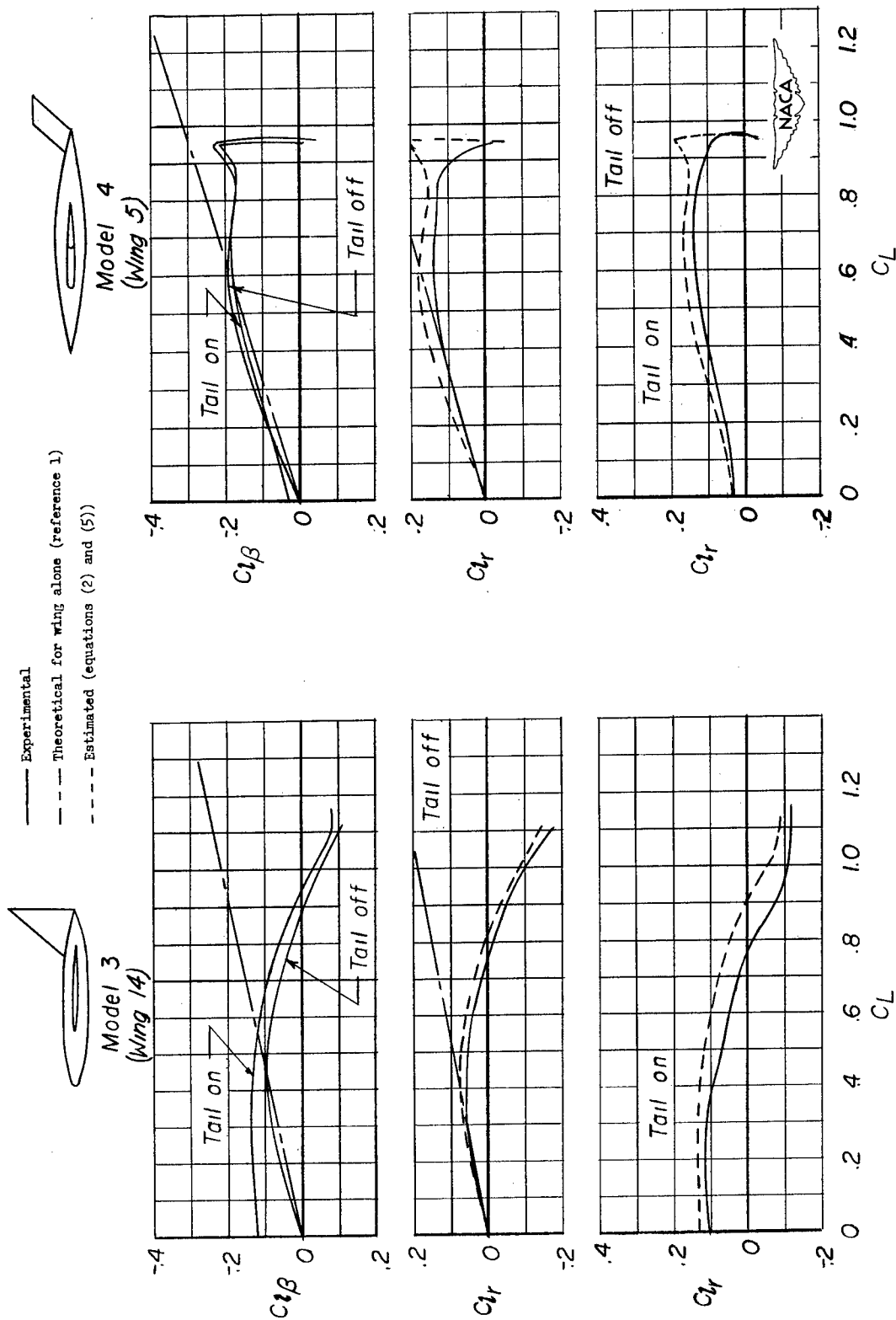Figure 15.- Estimation of the rolling moment due to yawing for models 1 and 2.

Figure 16.- Estimation of the rolling moment due to yawing for models 3 and 4.
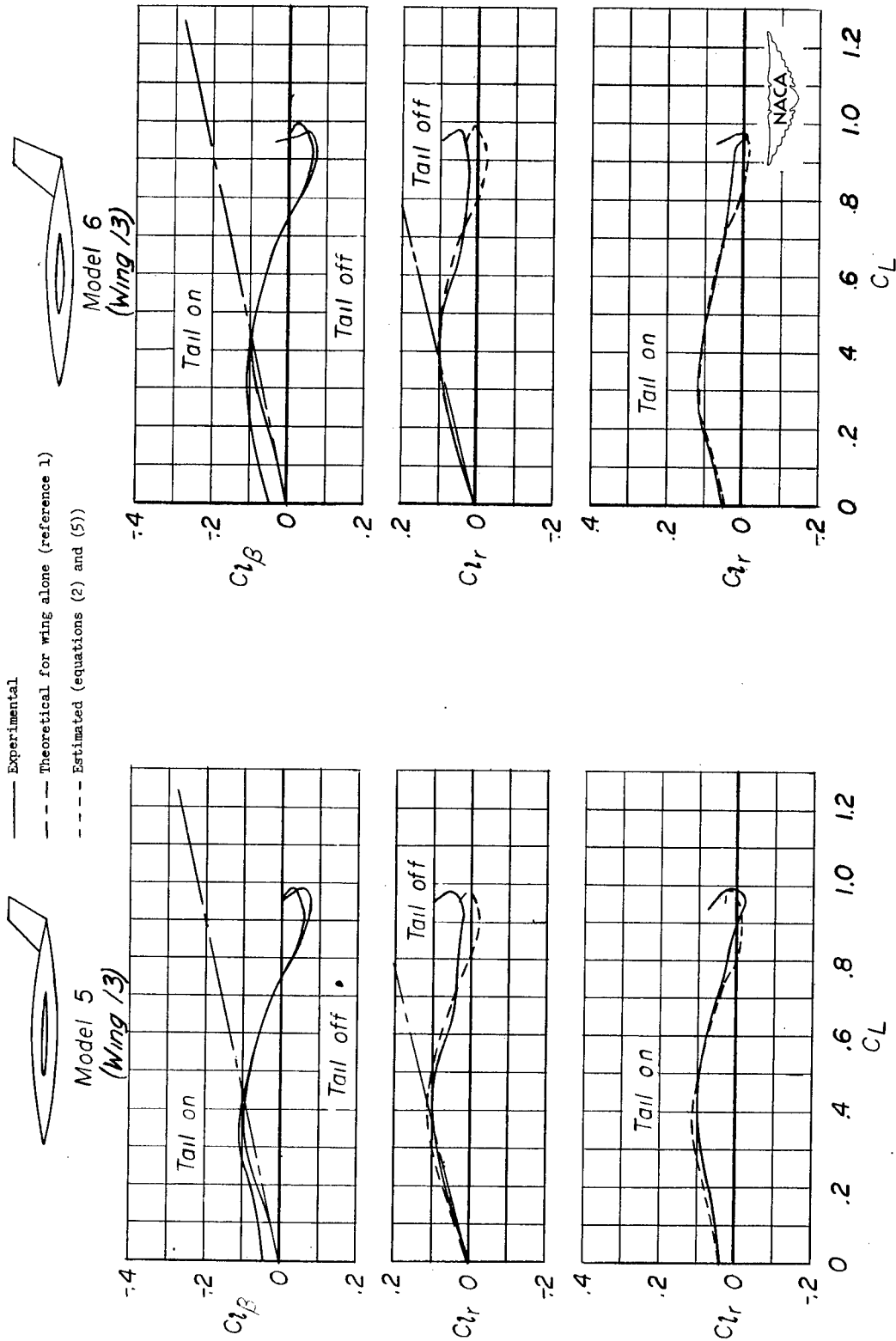
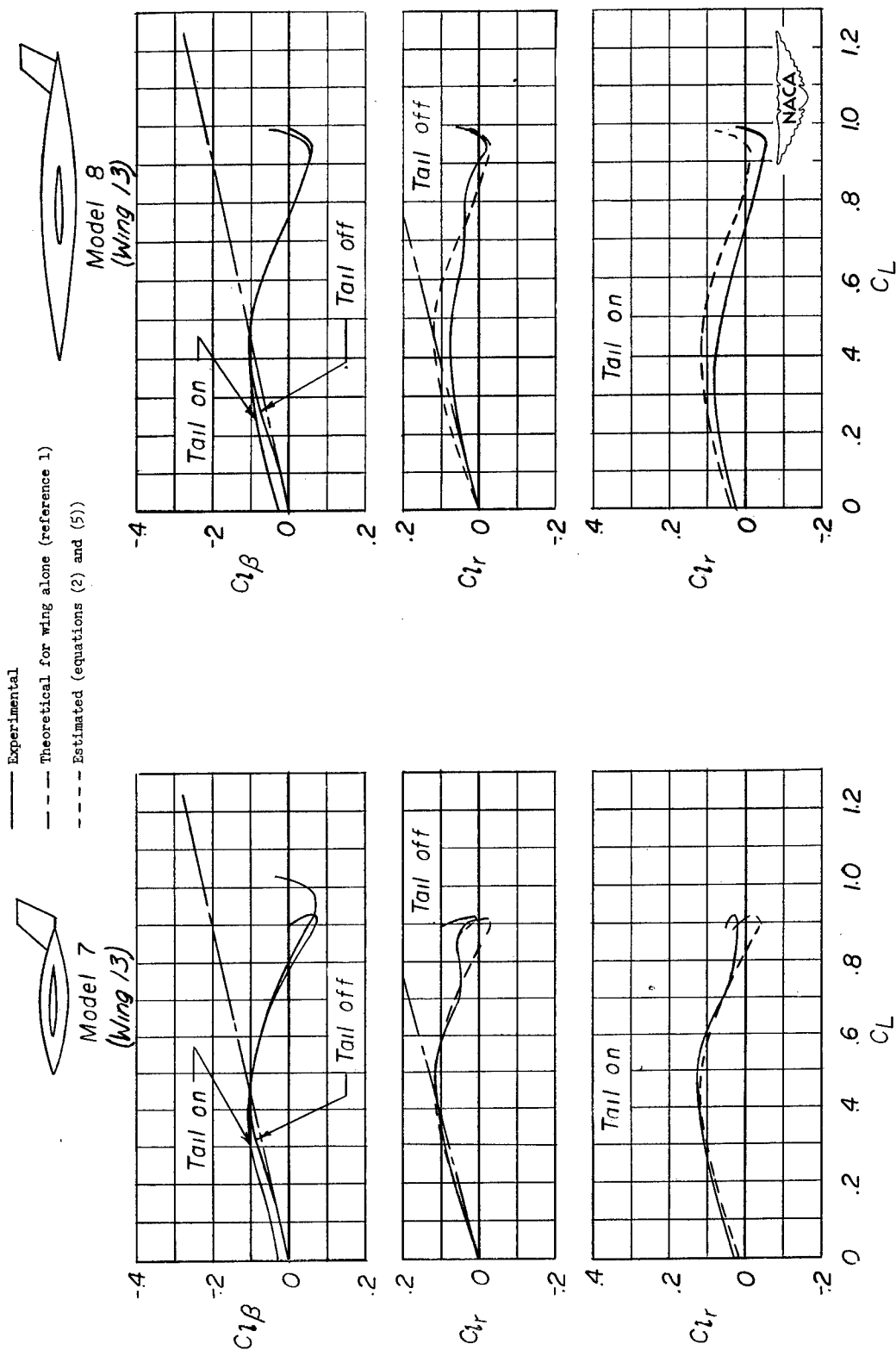Figure 17.- Estimation of the rolling moment due to yawing for models 5 and 6.

Figure 18.- Estimation of the rolling moment due to yawing for models 7 and 8.